Biomaterials 30 (2009) 1462–1472

Contents lists available at ScienceDirect

Biomaterials

journal homepage: www.elsevier.com/locate/biomaterials

Phospholipid decoration of microcapsules containing perfluorooctyl bromide used as ultrasound contrast agents

Raquel Díaz-López [a,b], Nicolas Tsapis [a,b,*], Danielle Libong [c], Pierre Chaminade [c], Carole Connan [d], Mohamed M. Chehimi [d], Romain Berti [e], Nicolas Taulier [e], Wladimir Urbach [e], Valérie Nicolas [f], Elias Fattal [a,b]

[a] Univ Paris Sud, UMR CNRS 8612, IFR 141, Faculté de Pharmacie, Châtenay-Malabry, France
[b] CNRS, UMR 8612, IFR 141, Faculté de Pharmacie, Châtenay-Malabry, France
[c] Univ Paris Sud, EA 4041, IFR 141, Faculté de Pharmacie, Châtenay-Malabry, France
[d] Univ Paris Diderot, ITODYS UMR CNRS 7086, Paris, France
[e] Univ Paris Sud, IFR141-ITFM, Plateau Technique-Imagerie Cellulaire, Châtenay-Malabry, France
[f] UPMC Univ Paris 06, CNRS UMR 7623, Laboratoire d'Imagerie Paramétrique, Paris, France

ARTICLE INFO

Article history:
Received 26 August 2008
Accepted 27 November 2008
Available online 20 December 2008

Keywords:
Microcapsules
Perfluorocarbons
Surface modification
Functionalization
Pegylated phospholipids
Biotinylated phospholipids

ABSTRACT

We present here an easy method to modify the surface chemistry of polymeric microcapsules of perfluorooctyl bromide used as ultrasound contrast agents (UCAs). Capsules were obtained by a solvent emulsification–evaporation process with phospholipids incorporated in the organic phase before emulsification. Several phospholipids were reviewed: fluorescent, pegylated and biotinylated phospholipids. The influence of phospholipid concentration on microcapsule size and morphology was evaluated. Only a fraction of the phospholipids is associated to microcapsules, the rest being dissolved with the surfactant in the aqueous phase. Microscopy shows that phospholipids are present within the shell and that the core/shell structure is preserved up to 0.5 mg fluorescent phospholipids, up to about 0.25 mg pegylated phospholipids or biotinylated phospholipids (for 100 mg of polymer, poly(lactide-*co*-glycolide) (PLGA)). HPLC allows quantifying phospholipids associated to capsules: they correspond to 10% of pegylated phospholipids introduced in the organic phase. The presence of pegylated lipids at the surface of capsules was confirmed by X-ray photon electron spectroscopy (XPS). The pegylation did not modify the echographic signal arising from capsules. Finally biotinylated microcapsules incubated with neutravidin tend to aggregate, which confirms the presence of biotin at the surface. These results are encouraging and future work will consist of nanocapsule surface modification for molecular imaging.

1. Introduction

Ultrasonic imaging is a widely available, non-invasive and cost-effective diagnostic modality, but the weak difference of echogenicity between different tissues often hampers a clear diagnostic. In order to better visualize specific tissues, ultrasound contrast agents (UCAs) are frequently used. Recently, ultrasound contrast agents consisting of gaseous perfluorocarbon bubbles encapsulated within polymer shells were developed [1]. The combination of a fluorinated gas, displaying a low solubility in blood and a biodegradable and non-toxic polymer, increased the plasmatic half-life of UCAs (>5 min) [2,3]. However, because these contrast agents are not stealth, they are quickly eliminated by the reticuloendothelial system [4]. In addition, UCAs also lack specificity and active targeting would be needed to image specific tissues. Surface modification of polymeric UCAs has been considered to enable both stealthiness and active targeting. Decorated with specific ligands, UCAs could target tumoral cells [2] allowing molecular imaging of angiogenic processes for example [5].

Novel polymeric contrast agents have been developed in our group [6,7]. These UCAs consist of microcapsules of poly(lactide-*co*-glycolide) acid (PLGA) encapsulating a liquid core of perfluorooctyl bromide (PFOB). The polymer was chosen because it has been approved by the FDA for use in sutures and drug delivery devices and several authors have reported that it is biodegradable and have good general biocompatibility [8]. The polymeric shell improved the stability of the capsules as compared to UCAs stabilized by a monomolecular layer [7]. However a major difficulty associated with coupling ligands to PLGA particles is the lack of sufficient functional chemical groups on the aliphatic polyester backbone. It severely hinders the application of traditional conjugation methods

* Correspondence to: Nicolas Tsapis, Univ Paris Sud, CNRS UMR 8612, Faculté de Pharmacie, 5 Rue Jean-Baptiste Clément, 92296 Châtenay-Malabry, France.
E-mail address: nicolas.tsapis@u-psud.fr (N. Tsapis).

0142-9612/$ – see front matter © 2008 Elsevier Ltd. All rights reserved.
doi:10.1016/j.biomaterials.2008.11.032

to the PLGA surface. Different approaches to introduce functionality into PLGA particles have been reported. The first approach consists of the synthesis of PLGA copolymers with polyethylene glycol (PEG) [9], poly(ε-caprolactone) (PCL) [9], or chitosan [10] which can be subsequently formulated into particles. This approach is however limited by the long and difficult synthesis of the copolymers. Another approach involves the blending or adsorption of functional polymers such as PEG, PCL [11,12], copolymers as poly(L-lysine)-*g*-poly(ethylene glycol) (PLL-*g*-PEG)[13] or polycationic polymers such as chitosan [14] or PEI [15], onto the preformed PLGA particles. This method is limited by the possible desorption of the adsorbed polymer which decreases the targeting effects.

In this paper, association of phospholipids to PLGA microparticles, as described by Fahmy et al. for fatty acids [16], was tested. Phospholipids conjugated with polyethylene glycol (PEG) and biotinylated-PEG were incorporated directly in the organic phase, before forming the microcapsules by solvent emulsion–evaporation. After evaporation phospholipid chains should preferentially partition into the hydrophobic PLGA matrix, whereas their hydrophilic head groups (PEG and PEG–biotin) should be oriented towards the hydrophilic external environment, facilitating the attachment of avidin ligands to the surface of microcapsules. Several phospholipids were reviewed: fluorescent phospholipids, pegylated phospholipids and biotinylated phospholipids, using the contrast agent developed in our laboratory [6,7].

2. Material and methods

2.1. Materials

Methylene chloride RPE-ACS 99.5% was purchased from Carlo Erba Reactifs (France). Chloroform and methanol were of HPLC-grade and purchased from VWR International (France). Acetic acid 99–100% RECTAPUR and ammonia solution at 32% RECTAPUR were purchased from VWR International (France). Water was purified using a RIOS system from Millipore (France). Poly(lactide-*co*-glycolide) acid 50:50, PLGA (Resomer RG502), was provided by Boehringer-Ingelheim (Germany). Sodium cholate (SC), Bovine Serum Albumin (BSA), streptavidin and Nile Red were obtained from Sigma–Aldrich. Perfluorooctyl bromide (PFOB) was purchased from Fluorochem. Phospholipids were provided as chloroform solutions by Avanti Polar Lipids Inc. (USA) (for abbreviations, see Table 1): L-α-Phosphatidylethanolamine-*N*-(lissamine rhodamine B sulfonyl), 1,2-dioleoyl-*sn*-glycero-3-phosphoethanolamine-*N*-(carboxyfluorescein), 1,2-distearoyl-*sn*-glycero-3-phosphoethanolamine-*N*-[methoxy(polyethylene glycol)-2000], 1,2-distearoyl-*sn*-glycero-3-phosphoethanolamine-*N*-[poly(ethylene glycol)2000-*N*′-carboxyfluorescein] and 1,2-distearoyl-*sn*-glycero-3-phosphoethanolamine-*N*-[biotinyl(polyethylene glycol)-2000]. Fluorescent streptavidin (Alexa Fluor 488), fluorescent neutravidin (Oregon green 488) and neutravidin were purchased from Invitrogen (France), as lyophilized powders and were reconstituted in phosphate buffer (PBS) at pH = 7.4.

2.2. Microcapsule preparation

Microcapsules were prepared by modifying the solvent emulsion/evaporation method for microspheres to obtain microcapsules with a polymeric shell encapsulating perfluorooctyl bromide (PFOB) [6]. Briefly, PLGA (0.1 g) was dissolved into 4 mL of methylene chloride along with 60 μL of PFOB and the desired amount of phospholipids dissolved into chloroform. The organic solution was placed in a thermostated bath maintained at 20 °C to ensure full miscibility of the PFOB. It was then emulsified into 20 mL of 1.5% sodium cholate (w/v) aqueous solution using an Ultra-turrax T25 (IKA) operating with an SN25-10G dispersing tool at a velocity of 8000 rpm. Emulsification was performed in a 50 mL beaker placed over ice. Methylene chloride and chloroform were then evaporated by magnetic stirring for about 3 h at 300 rpm in a thermostated bath (20 °C). After full evaporation of the solvents, the suspension volume was completed to 20 mL with water in a volumetric flask. For fluorescent or confocal microscopy, Nile Red was added to the organic solution prior to emulsification. Typically, about 100 μL of a concentrated Nile Red solution (0.057 mg/mL in methylene chloride) was added to the organic solution. Microcapsules were washed by centrifugation (2000*g*, 10 min, 4 °C) (MR 1812 centrifuge, Jouan, France). The supernatant containing the surfactant was discarded and microcapsules were resuspended with water (5 mL) by vortexing (30 s). Plain microcapsules will be abbreviated MC, pegylated microcapsules MC-PEG and biotinylated microcapsules MC-Biot in the rest of the article. After full evaporation of the solvents, the suspension volume was completed to 20 mL with Milli-Q water in a volumetric flask and fresh microcapsules were frozen at −20 °C. Samples were then freeze-dried for 48 h using an LYOVAC GT2.

Table 1
Characteristics of the phospholipids used for capsule surface modification.

Types of phospholipids	Abbreviation	Chemical name
Fluorescent phospholipid, Red	PE-Rhod	L-α-Phosphatidylethanolamine-*N*-(lissamine rhodamine B sulfonyl)
Fluorescent phospholipid, Green	PE-CF	1,2-Dioleoyl-*sn*-glycero-3-phosphoethanolamine-*N*-(carboxyfluorescein)
Pegylated phospholipid	DSPE-PEG	1,2-Distearoyl-*sn*-glycero-3-phosphoethanolamine-*N*-[methoxy (polyethylene glycol)-2000]
Fluorescent pegylated phospholipid	DSPE-PEG-CF	1,2-Distearoyl-*sn*-glycero-3-phosphoethanolamine-*N*-[poly(ethylene glycol)2000-*N*′-carboxyfluorescein]
Biotinylated phospholipid	DSPE-PEG-biotin	1,2-Distearoyl-*sn*-glycero-3-phosphoethanolamine-*N*-[biotinyl(polyethylene glycol)-2000]

2.3. Streptavidin/neutravidin coupling to the biotinylated microcapsules

To prove that the biotin groups of the biotinylated phospholipids were present at the microcapsule surface, the high ability of streptavidin/neutravidin to bind 4 biotins was used [17]. 100 μL of biotinylated microcapsules were first incubated with 1 mL of a BSA solution (1 mg/mL) for 30 min at 37 °C under tangential agitation, to reduce non-specific binding. To eliminate the unbound BSA, samples were centrifuged (10 min at 12,000*g*, centrifuge Mini Spin, Eppendorf) and pellets were resuspended with 1 mL of PBS pH = 7.4 by vortexing (30 s). These samples were then incubated for 30 min at 37 °C under tangential agitation with different amounts of streptavidin or neutravidin. The streptavidin used was fluorescent, Alexa Fluor 488, a volume of 50 μL at 1 mg/mL (equivalent at 9.5×10^{-7} mmol of streptavidin). In the case of neutravidin non-fluorescent was used for the incubations in a range between 5 μL and 65 μL at 5 mg/mL (equivalent at 2.08×10^{-7}–2.71×10^{-6} mmol of neutravidin). For fluorescent neutravidin with Oregon green 488, volumes of 5 μL and 10 μL at 1 mg/mL were used.

2.4. Size distribution

Size measurements on microcapsules were performed by laser diffraction, using an LS230 Particle Size Analyzer (Coulter-Beckmann). Size distribution was analyzed using the Mie theory. Before each measurement, 200 μL of microcapsule suspension were diluted into 1 mL of Milli-Q water and ten drops were added to water in the sample cell. Measurements were performed in triplicate at room temperature. Data obtained were expressed in terms of the particle diameter at 10%, 50% and 90% of the volume distribution (D_{10}, D_{50} and D_{90}, respectively) and as the mean particle diameter. The uncertainty of the measurement was around 1%.

2.5. Optical and fluorescence microscopy

Capsule suspension was placed between glass slides and observed with a Leitz Diaplan microscope equipped with a Coolsnap ES camera (Roper Scientific). Fluorescent samples dyed with Nile Red were excited at 543 nm and observed at 560 nm (long-pass filter). Fluorescent samples dyed with fluorescein or with Oregon green were excited at 488 nm and observed at 510 nm.

2.6. Confocal laser scanning microscopy (CLSM)

Glass slides were examined with a Zeiss LSM-510 confocal scanning laser microscope equipped with a 30 mW argon laser and 1 mW helium neon laser, using a Plan Apochromat 63× objective (NA 1.40, oil immersion). Red fluorescence was observed with a long-pass 560 nm emission filter and under a 543 nm laser illumination. Green fluorescence was observed with a band-pass 505 and 550 nm emission filter and under a 488 nm laser illumination. The pinhole diameter was set at 71 μm. Stacks of images were collected every 0.42 μm along the *z* axis.

2.7. Scanning electron microscopy (SEM)

Scanning electron microscopy was performed using a LEO 1530 (LEO Electron Microscopy Inc., Thornwood, NY) operating between 1 and 3 kV with a filament current of about 0.5 mA. Liquid samples were deposited on carbon conductive double-sided tape (Euromedex, France) and dried at room temperature. They were coated with a palladium–platinum layer of ca. 4 nm using a Cressington sputter-coater 208HR with a rotary-planetary-tilt stage, equipped with an MTM-20 thickness controller. Particles were washed by centrifugation before imaging, as indicated previously, to remove the excess amount of surfactant that reduces the quality of the images.

2.8. Quantification of DSPE-PEG associated to microcapsules

Three independent preparations of MC-PEG were prepared, each one with a different volume of pegylated lipids at 440 mg/mL in chloroform: 100, 300 and 500 μL. For each preparation of MC-PEG the total, free and associated DSPE-PEG2000 were quantified. For the quantification of total pegylated phospholipids, microcapsules after their fabrication were frozen at −20 °C and then freeze dried for 48 h using an LYOVAC GT2. In the case of free and associated pegylated phospholipids, MC-PEG was separated from the aqueous solution containing the free phospholipids and the surfactant by centrifugation (2000g, 10 min, 4 °C) (MR 1812 centrifuge, Jouan, France). Microcapsules were resuspended with water (5 mL) by vortexing (30 s). Then microcapsules and supernatants were frozen separately and freeze dried in the same conditions. Freeze-dried pellets of microcapsules were dissolved by adding first 2 mL of chloroform followed by 1 mL of methanol. Volumes of chloroform and methanol used to dissolve the freeze-dried pellets of supernatant were adjusted according to the initial concentration of DSPE-PEG in the sample. For example, the preparation obtained with 100 mL DSPE-PEG (at 440 mg/mL), volumes were 2 mL and 1 mL (chloroform and methanol), whereas the one obtained with 300 mL the volumes were 7.8 mL and 3.9 mL. Solutions were filtered on a 0.22 μm PTFE filter prior to injection and analysis. The quantification was determined by high performance liquid chromatography (HPLC) with a Charged Aerosol Detection (CAD). The chromatographic system consisted of a Hewlett Packard HP 1050 pump with Rheodyne manual injection valve, a 100 μL sample loop and a Zorbax Eclipse XDB-C8 column (150 mm × 4.6 mm, I.D. 5 μm). Detection was performed with the corona CAD, a charged aerosol detector (ESA Biosciences, USA), the sensitivity was 200 pA, the air pressure was of 35 psi with a "medium filter" setting. The mobile phase consisted of acetonitrile, methanol, ammonia and acetic acid (84.63:15:0.26:0.11, v/v/v/v) (phase A) and methanol, ammonia and acetic acid (99.63:0.26:0.11, v/v/v) (phase B). The different components of MC and MC-PEG were separated by running a gradient starting at 100% mobile phase A, decreasing to 40% A in 9 min and then back to 100% A in 1 min and finally isocratic condition 100% A for 10 min [18].

2.9. X-ray photoelectron spectroscopy (XPS) analysis

Specimens were pressed against double-sided adhesive tapes on sample holders and pumped overnight in the fast entry lock at $\sim 5 \times 10^{-8}$ mbar. XPS spectra were recorded with a Thermo VG Scientific ESCALAB 250 spectrometer (East Grinstead, UK) equipped with a monochromatic Al Kα X-ray source (1486.6 eV, 650 μm spot size). The pressure in the analysis chamber was *ca.* 2–3 $\times 10^{-8}$ mbar. The pass energy was set at 150 and 40 eV for the survey and the narrow scans, respectively. The step size was 1.0 eV for the survey spectra and 0.1 for the narrow regions, respectively. Charge compensation was achieved with an electron flood gun operated in the presence of argon at a partial pressure of 2×10^{-8} mbar in the analysis chamber. In these conditions, the surface charge was negative but perfectly uniform. Data acquisition and processing were achieved using Avantage software, version 3.51. The surface composition was determined using the manufacturer's sensitivity factors. The fractional concentration of a particular element A (% *A*) was computed using $\%A = (I_A/S_A)/(\sum(I_n/S_n)) \times 100$, where I_n and S_n are the integrated peak areas and the sensitivity factors, respectively. The internal calibration method was chosen for spectral calibration, leading to set the $C_{C-C/C-H}$ component at 285 eV.

2.10. In vitro echogenicity

Suspensions of microcapsules in Milli-Q water at different concentrations (5, 10, 15, 20, 30, 40 and 50 mg/mL) were placed in a 3-mm-deep, cylindrical, stainless steel chamber. The top of the chamber was sealed with an acoustically transparent cellophane membrane. At its bottom, a small 1-mm-deep cylindrical cavity allowed a magnetic stir bar to agitate the suspension without disturbing the signal (Fig. 1). The chamber was immersed into water and insonified along an axis perpendicular to its bottom by a polyvinylidene fluoride broadband transducer (model PI 75-1, Panametrics Inc., USA). The transducer was positioned so that its focus was inside the solution, close to the cellophane membrane. During the experiment, the transducer emitted one short ultrasound pulse at a repetition rate of 1 kHz using a Panametrics Sofranel 5900 PR emitter/receiver. The pulse duration was 0.08 μs at −20 dB of the negative peak value, and the −6 dB band-pass ranges from 40 to 60 MHz. The backscattered ultrasound signal was received by the same transducer, digitized at a sampling rate of 400 MHz on a digital oscilloscope (model 9450A, Lecroy, USA) and transferred to a personal computer for signal processing using MATLAB©. Experiments performed on either MC or MC-PEG suspensions provide the signal $s_{suspension}(t)$, whereas experiments performed on sodium cholate solution as a reference give $s_{reference}(t)$. We derived $S(\upsilon)$: the Fast Fourier Transform applied on the temporal signal $s(t)$, in a 530 points Hamming window corresponding approximately to 1.98 mm depth beginning at the transducer focus. The Power Spectrum Density is then defined as: $PSD = |S(\upsilon)|^2$ and the Signal-to-Noise Ratio (SNR) was calculated as: $SNR = 10 \log(PSD_{suspension}/PSD_{reference})$, where $PSD_{suspension}$ and $PSD_{reference}$ are the PSD derived from the suspension and from the reference, respectively. The SNR measures the contrast enhancement and was averaged over 15 measurements.

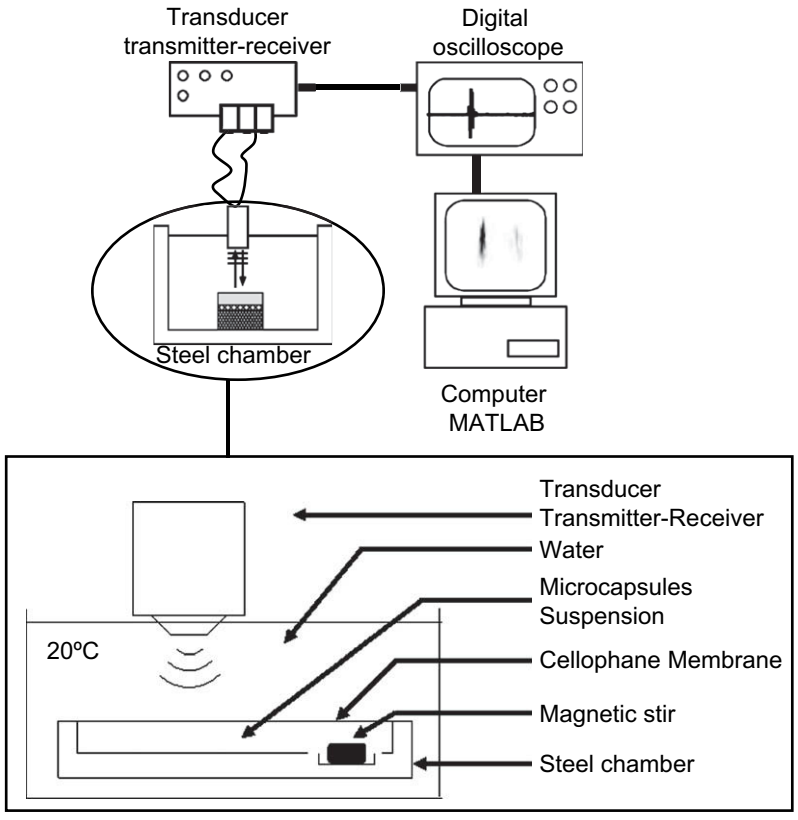

Fig. 1. Scheme of the experimental set up for *in vitro* echogenicity measurements.

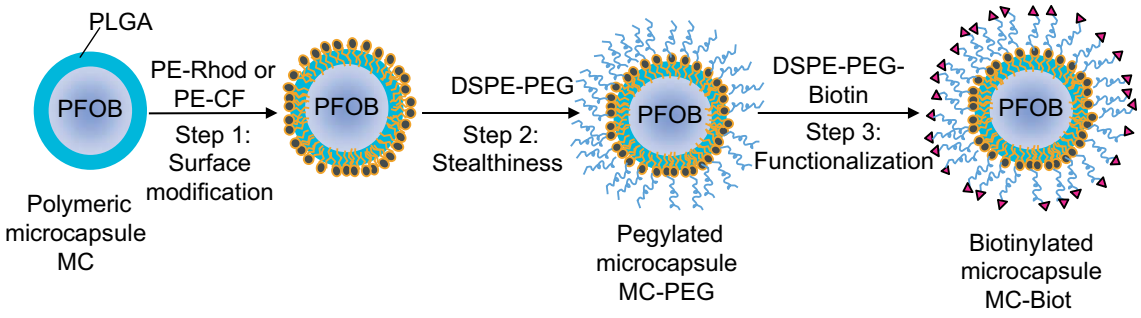

Fig. 2. Overall scheme of the different types of microcapsule surface modification.

3. Results and discussion

The aim of this paper was to modify the surface of polymeric microcapsules used as ultrasound contrast agent, in order to make the capsules bind to endothelial cells or tumor neovessels. The overall scheme of the different steps for surface modification and functionalization is shown in Fig. 2. The different steps were first to use fluorescent phospholipids to ascertain their association to microcapsules, then to replace fluorescent phospholipids by pegylated phospholipids and finally to use biotinylated phospholipids. Although small particles are required to achieve stealthiness, our work has focused on large capsules in order to observe morphological changes. Indeed, we have previously demonstrated that switching from microcapsules to nanocapsules does not modify neither the capsule morphology nor the thickness to radius ratio [6,19].

3.1. Surface modification of microcapsules by fluorescent phospholipids

The ability to cover homogenously the surface of the microcapsules with phospholipids without losing the core–shell morphology was first evaluated. Fluorescent phospholipids were used and added to the organic phase with the PLGA before

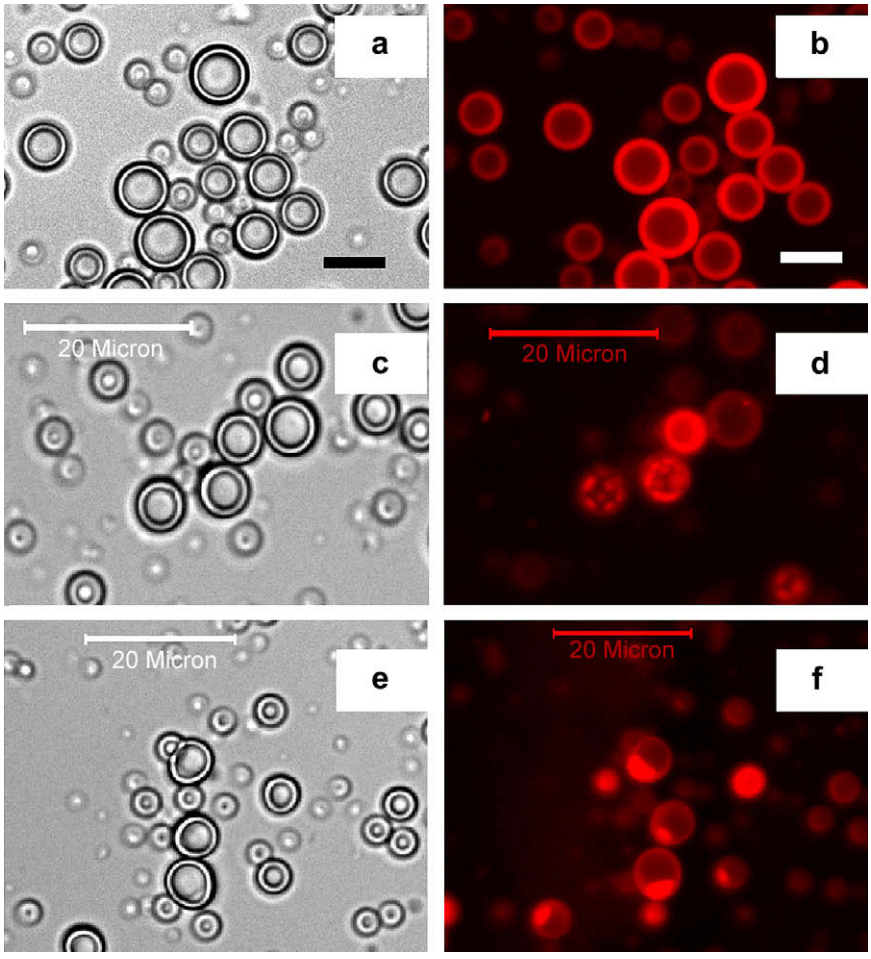

Fig. 3. Microscopy images of a suspension of microcapsules with PE-Rhod. Bright field is presented on the left, whereas fluorescence is on the right (the polymer appears bright, and the PFOB appears dark). Scale bars represent 5 μm in top images and 20 μm in middle and bottom images. (a)–(b) with 0.1 mg, (c)–(d) with 0.5 mg, (e)–(f) with 1 mg of PE-Rhod in the organic phase.

Table 2
Size distribution of microcapsules as a function of the amount and type of phospholipids. The uncertainty was around 1%.

Phospholipids	Amount[a] (μg)	Mean	Diameter (μm)		
			D_{10}	D_{50}	D_{90}
None	0	6.0	1.5	6.6	9.5
PE-Rhod	1.8	6.1	1.5	6.6	9.7
	3.6	6.1	1.5	6.6	9.7
	5	6.1	1.5	6.7	9.6
	20	6.1	1.5	6.5	9.7
	40	6.1	1.5	6.5	9.7
	52	5.8	1.4	6.3	9.2
	100	5.7	1.4	6.3	9.1
	120	6.3	1.4	6.4	9.3
	500	5.3	1.2	5.7	8.8
DSPE-PEG	2.6	6.6	1.5	6.6	9.6
	5.7	6.2	1.5	6.8	9.8
	28.6	9.3	1.5	6.7	10.8
	57.2	5.9	1.4	6.5	9.5
	264	6.3	1.4	6.4	9.3
DSPE-PEG-biotin	62.5	6.1	1.3	6.5	10.0
	125	7.0	1.4	6.8	10.4
	250	6.2	1.4	6.7	9.9

[a] In the organic phase.

emulsification. Since capsules are denser than water due to the PFOB core, they sediment rather fast. After sedimentation, we have noticed that both the pellet and the supernatant were red. This indicates that a certain amount of fluorescent phospholipids is not associated to microcapsules. They are probably solubilized by sodium cholate used for emulsification. Indeed, this bile salt is known to be a good solubilizer of phospholipids, forming micelles or eventually vesicles [20]. With 2 μg PE-Rhod (for 100 mg PLGA), bright field and confocal microscopy shows that the core–shell structure of the microcapsules is not modified. As phospholipid concentration increases between 2 μg and 1 mg PE-Rhod bright field and fluorescent microscopy reveals that microcapsules' morphology is preserved until 0.5 mg of PE-Rhod (Fig. 3). Microcapsule shells are clearly visible on the optical microscopy images and by fluorescence microscopy where phospholipids appear red whereas PFOB core appears dark. Up to an amount of 0.1 mg of PE-Rhod, spherical capsules with a nice red shell of homogeneous thickness and a darker core were observed by fluorescence microscopy (Fig. 3, a–b). For about 0.5 mg PE-Rhod, the capsule morphology is preserved but the repartition of the fluorescence is modified (Fig. 3, c–d). Fluorescent spots are observed on some microcapsules. Phospholipids form zones of major density in some parts of the surface. Similar observations were performed by Ladavière et al. [21]. We can interpret these observations as a phase separation between zones rich and poor in phospholipids at the microcapsule surface. A saturation of the polymer by the lipids could explain the phase separation. Starting from 1 mg PE-Rhod, morphological changes appear. Some capsules conserve a core–shell structure, while others have an "acorn" morphology with a very fluorescent hemisphere (Fig. 3, e–f). In this case, we also observe a phase separation between a rich and poor zone of lipids. Most probably, lipidic spots observed for 0.5 mg of lipids merge when the amount of lipid increases. These changes may arise from modifications of the interfacial tensions induced by phospholipids during solvent evaporation as already observed by Pisani et al. for surfactants [19].

The size distribution was also measured as a function of the amount of fluorescent phospholipids added in the organic phase (Table 2) for microcapsules with a preserved core–shell structure. The mean size of decorated capsules was around 6 μm, similar to the plain capsules in the range between 1.8 μg and 0.5 mg of PE-Rhod for 100 mg PLGA.

Surprisingly, phospholipids are not preferentially localized at the polymer/water interface. In fact, the fluorescence observed in confocal microscopy is homogenous, in all the shell thickness. Some lipids are at the polymer/water interface but others seem to be mixed within the polymer shell. To further verify phospholipid distribution in microcapsules, Nile Red was added as a fluorescent marker, to stain the hydrophobic polymer and PE-Rhod was substituted by green fluorescent phospholipids, PE-CF. Microcapsule suspensions were observed by confocal microscopy (Fig. 4). The core–shell structure of the microcapsules is perfectly observable; the shell is well defined and appears in red, while the lipids appear in green. When the two images are superimposed, both colors overlap perfectly. Despite solubilization of lipids by sodium cholate, some of them are at microcapsule surface and others are associated to the bulk of the polymeric shell.

3.2. Microcapsules modified by pegylated phospholipids

The second step of the schematic process of surface modification of our polymeric microcapsules consists of pegylating their surface. Pegylation is indeed needed, since after intra-venous injection [3], due to their rather hydrophobic surface, these UCA candidates would quickly be eliminated by the reticuloendothelial system and end up in macrophages in the liver or the spleen. To avoid a rapid clearance from the systemic circulation, it has been shown that covering particle's surface with poly(ethylene glycol) (PEG) is very efficient [22]. By its hydrophilic nature PEG provides protection from blood protein adsorption, and uptake by the reticuloendothelial system is drastically reduced [23]. Furthermore, PEG is non-toxic, safe and has a good biocompatibility [24]. In order to prepare microcapsules covered with PEG, a pegylated phospholipid DSPE-PEG was added in the organic phase prior to emulsification. As for the surface modification with fluorescent lipids, the morphology, size and localization of phospholipids were studied as function of the amount of DSPE-PEG added in the formulation.

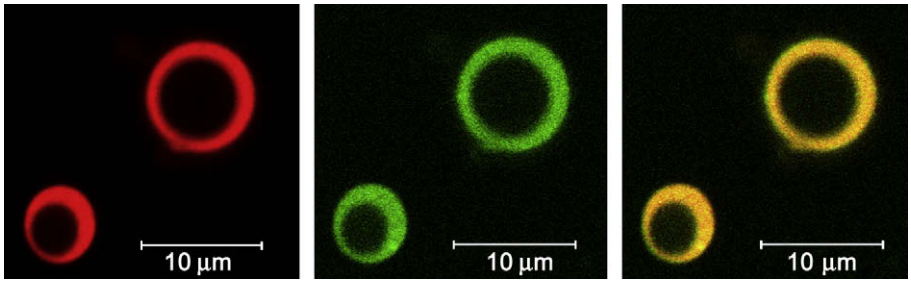

Fig. 4. Confocal microscopy images (scale bar = 10 μm) of a suspension of microcapsules with 100 μg of PE-CF. PLGA is dyed in red (left), lipids appear in green (center) and superposition of both images (right).

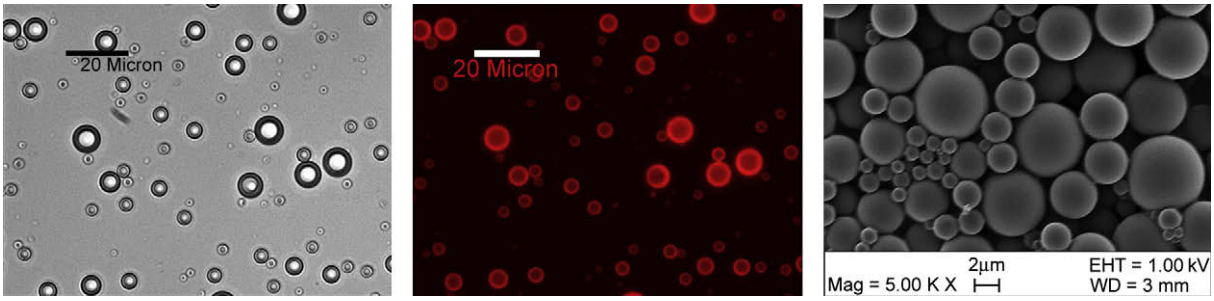

Fig. 5. Images of suspensions of MC-PEG prepared with 264 µg DSPE-PEG (left: bright field, center: fluorescent microscopy, right: SEM). Scale bars represent 20, 20 and 2 µm from left to right.

3.2.1. Effect of DSPE-PEG amount on microcapsule morphology and size distribution

The range of DSPE-PEG added in the organic phase varied between 2.6 µg and 440 µg of DSPE-PEG. As for PE-Rhod decorated microcapsules the core–shell morphology is preserved up to a certain concentration of phospholipids. Optical and fluorescent microscopy images (Fig. 5) show that until 264 µg of DSPE-PEG, the microcapsule core–shell structure remains unchanged. Beyond 264 µg DSPE-PEG, "acorn" morphologies as those observed with PE-Rhod were visualized by microscopy. Despite DSPE-PEG is not fluorescent, the modification of the core–shell morphology when phospholipid concentration increases proves that phospholipids are indeed associated to capsules. The size of MC-PEG did not change significantly with increasing amounts of DSPE-PEG, the mean diameter is around 6.6 µm (Table 2), similar as MC and PE-Rhod microcapsules. To ascertain that DSPE-PEG was indeed associated to microcapsule's shell, fluorescently labeled pegylated phospholipids, DSPE-PEG-CF, were used, along with Nile Red as a marker for PLGA. Microcapsule suspensions were examined by confocal microscopy, after centrifugation to eliminate free fluorescent phospholipids, green fluorescence could be observed within the shell. The green fluorescence superimposes perfectly with the red one arising from Nile Red unless capsules have moved (Fig. 6). Despite solubilization of some phospholipids by sodium cholate, a fraction of pegylated phospholipids remains associated to microcapsules either at their surface or mixed with the polymer shell. Quantification of lipids associated to microcapsules or solubilized along with the surfactant is of major importance to estimate if our method allows covering microcapsule surface efficiently. In addition, once capsules have been washed, fluorescence remains associated to microcapsules even in the presence of surfactant, until the polymer starts to degrade: the surface modification is therefore rather stable.

3.2.2. Surface characterization of pegylated microcapsules

SEM observations reveal microcapsules with a spherical shape and a smooth surface (Fig. 5). DSPE-PEG does not induce any surface porosity or roughness. XPS was used to get information on the elemental and chemical compositions of particle surface within a depth of ~10 nm, much smaller than microcapsule shell thickness which is around 1 µm. It was expected that XPS could be used to distinguish between MC and MC-PEG.

The apparent surface elemental compositions (in atomic percent) of the specimens as determined by XPS are reported in Table 3. Besides C and O, N and P were detected in the analysis of DSPE-PEG since this phospholipid bears an ammonium counter-ion. For MC, the O/C ratio is equal to 0.70 matching the value of 0.69 determined for PLGA. This proves that MC has a PLGA-rich surface.

For MC-PEG, the elemental composition is almost identical to that of DSPE-PEG. Particularly the O/C ratio is 0.26 for the former matching 0.25 for the latter. These observations confirm that MC-PEG has a phospholipid-rich surface.

In order to get a deeper insight of the surface chemical compositions of MC-PEG and reference materials, the high resolution C1s and O1s regions were recorded and peak-fitted. Fig. 7 displays the peak-fitted C1s and O1s regions of MC, DSPE-PEG and MC-PEG; those due to PLGA are not shown as they are almost identical to those of MC. The peak fitting parameters are displayed in Table 4. For MC, the C1s peak is fitted with three components centered at 285, 286.9 and 289.1 eV corresponding to C–C/C–H bonds, C–O and O–C=O, respectively, in the ~1:1.2:1.6 ratios matching the theoretical ones calculated for PLGA. The O1s region is fitted with two components centered at 532.2 and 533.7 eV corresponding to C=O and C–O–C, respectively, with a 1:1.3 ratio. The shape and fitting of the O1s region from MC are also similar to those of PLGA. This is an indication that MC surface consists essentially in PLGA.

In the case of DSPE-PEG, the C1s and O1s spectra markedly differ from those of MC (and thus from the PLGA shell). The C1s peaks are fitted again with three components centered at 285, 286.4 and 289 eV corresponding to C–C/C–H, C–O and O–C=O bonds. The main difference in the C1s fine structure lies in the steep increase in the ratio of the C–O to the ester C1s components. Indeed, while PLGA has an ester-rich composition (39.1% of ester carbon),

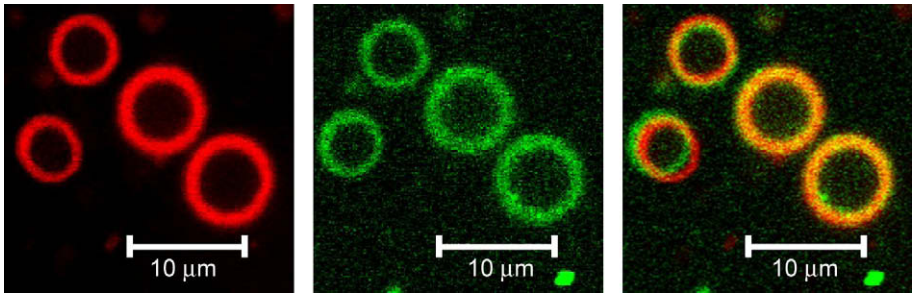

Fig. 6. Confocal microscopy images (scale bar = 10 µm) of a suspension of microcapsules prepared with 50 µg of DSPE-PEG-CF. PLGA is dyed in red (left), lipids appear in green (center) and superposition of both images (right).

Table 3
Apparent surface elemental composition as determined by XPS.

Sample	XPS elemental ratios (%)			
	C	O	N	P
PLGA	59.0	41.0	–	–
MC	58.9	41.1	–	–
DSPE-PEG	78.2	19.7	0.84	1.16
MC-PEG	79.2	20.4	–	–

phospholipids have on the contrary a PEG-rich composition and thus an important contribution of C–O bonds (40.5%); these bonds induce a C1s component centered at ~286.4 eV. In the case of the DSPE-PEG, one can also clearly see the long alkyl chains C–C/C–H bonds which contribute a component at 285 eV. Interestingly, the ester and carbamate groups from the phospholipids induce a small peak at 289–290 eV. For the sake of simplicity, the C1s components corresponding to these functional groups are lumped together in one single peak centred at ~289 eV.

The O1s region of DSPE-PEG is fitted with two components centered at 531.3 and 532.8 eV corresponding to oxygen atoms in the phosphate group [25] and in the PEG chain [26], respectively. Note that the O1s signals corresponding to N–C=O and O–C=O in the DSPE-PEG are lumped with the main component which is dominated by PEG.

In the case of the MC-PEG, the C1s region exhibits a fine structure that resembles DSPE-PEG structure, however with a lower contribution of the C–O C1s component at ~286 eV. Nevertheless, the C–O/ester intensity ratio is still higher for MC-PEG than MC. The O1s region also has a composite structure of the PLGA and DSPE-PEG; it is fitted with three components assigned to mostly phosphate (I), PEG and C=O (II), and O–C=O (III), respectively. These C1s (Fig. 7E) and O1s (Fig. 7F) regions testify for a PEG-rich surface of the MC-PEG capsules.

3.2.3. Quantification of DSPE-PEG associated to microcapsules

The total DSPE-PEG in the whole suspension, the free DSPE-PEG in the supernatant and the pegylated phospholipids associated to microcapsules were quantified in 3 batches with different amount of pegylated phospholipids as described in detail elsewhere [18]. Keeping constant the polymer (PLGA), the amount of DSPE-PEG associated to the microcapsules increases with increasing amounts

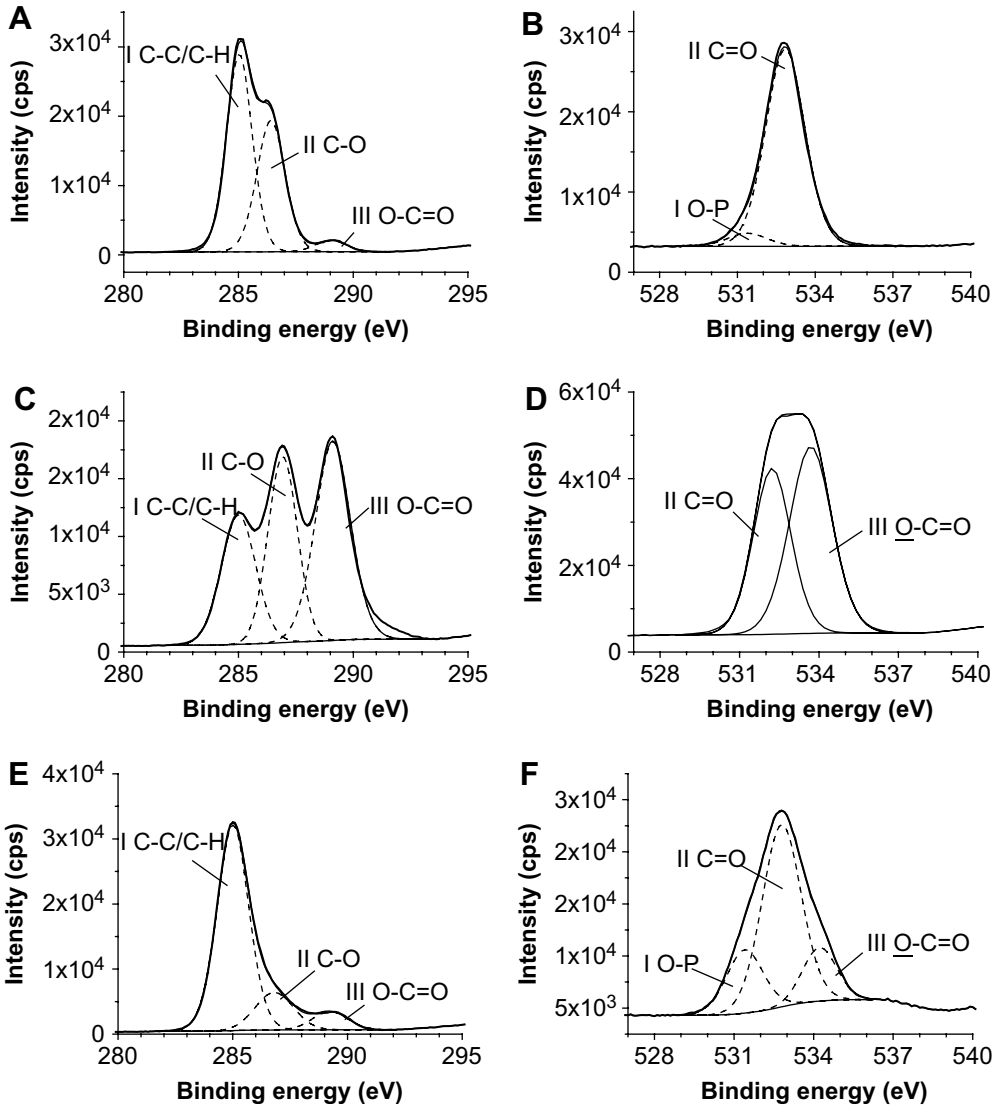

Fig. 7. High resolution XPS spectra of DSPE-PEG (A and B) MC (C and D) and MC-PEG (E and F). Graphs on the left present C1s regions whereas graphs on the right present O1s regions. Full lines correspond to experimental data, whereas dashed lines correspond to fittings.

Table 4
C1s and O1s peak fitting parameters for PLGA, MC, DSPE-PEG and MC-PEG.

Sample	Peaks binding energy (eV) C1s			Peaks binding energy (eV) O1s		
	I (C–C/C–H)	II (C–O)	III (O–C=O)	I (O–P)	II (C=O)	III (O–C=O)
PLGA	285.0 (23.3%)	286.9 (37.6%)	289.1 (39.1%)		532.4 (45.8%)	533.9 (54.2%)
MC	285.0 (26.3%)	286.9 (32.0%)	289.1 (41.7%)		532.2 (44.0%)	533.7 (56.0%)
DSPE-PEG	285.0 (55.7%)	286.4 (40.5%)	289.0 (3.8%)	531.3 (6.2%)	532.8[a] (93.8%)	–
MC-PEG	285.0 (76.1%)	286.1 (16.5%)	289.2 (7.4%)	531.4 (20.7%)	532.8[a] (63.2%)	534.2 (16.1%)

[a] The main O1s component is due to C–O bonds in PEG. Note that the binding energies are lower than those observed for polyacrylates or polymethacrylates but match typical binding energies reported for oxygen atoms in O–C=O.

of DSPE-PEG (Table 5). This is also the case for free phospholipids in the supernatant. Independent of the initial DSPE-PEG concentration, approximately 10% of the initial phospholipids are associated to microcapsules whereas the remaining 90% are free in the supernatant (Table 5). Despite their solubilization by the surfactant, a minimum of 1.83 ± 0.8 μg of DSPE-PEG is present for 100 mg of polymer used.

The number of pegylated phospholipids present at the surface of microcapsules was calculated, considering that 10% of the initial amount of phospholipids is associated to microcapsules and that all the molecules are present at the surface. Microcapsule surface (S_{MC}) was calculated, taking into account a microcapsule mean diameter (D) equal to 6 μm: $S_{MC} = \pi D^2 = 1.13 \times 10^{-10}$ m^2. The specific surface area (S_{sp}) of the microcapsule suspension is $S_{sp} = 6/D\rho$, where ρ is the density (1.5 g/cm^3) [6], giving $S_{sp} = 0.667$ m^2 g^{-1}. For a typical preparation, the available surface is therefore $S_{sp} \times 0.18$ g $= 0.12$ m^2. The number of microcapsules (N_{MC}) in a typical suspension of 0.18 g [6] is then given by $N_{MC} = 0.18 \times S_{sp}/S_{MC} = 1.06 \times 10^9$. The maximum number of pegylated lipids ($N_{PEG\text{-}Lip}$) in a preparation is $N_{PEG\text{-}Lip} = (m_{DSPE\text{-}PEG}/M_{DSPE\text{-}PEG})\ N = 4.75 \times 10^{15}$, where $M_{DSPE\text{-}PEG}$ is the molecular weight of DSPE-PEG (2787.49 g/mol) and N the Avogadro number. If one divides the available surface in the preparation by the number of phospholipids, one finds that 25 nm^2 are available for each PEG chain. Although, 25 nm^2 is not the optimal 2 nm^2 for maximal reduction of protein adsorption [9], it might lead to sufficient protection from large protein adsorption.

3.2.4. *In vitro* echogenicity of pegylated microcapsules

We have verified that the surface modification with DSPE-PEG did not change the ultrasonic properties of microcapsules. MC-PEG prepared with 0.22 mg DSPE-PEG in the organic phase was compared with MC previously evaluated *in vitro* from an ultrasonic point of view. Considering that the size of the microcapsules is around 6 μm, a concentration of 50 mg/mL corresponds to about 4×10^8 microcapsules per milliliter [7]. The *in vitro* echogenicity of MC-PEG and MC was compared as a function of concentration at 50 MHz in a pulse echo-mode (Fig. 8). The signal-to-noise ratio (SNR) was measured for both systems. As microcapsule concentration increases, the SNR increases until it reaches a maximum around 15 dB, similar to the plateau value obtained by Pisani et al. [7]. There are no significant differences of the SNR between MC and MC-PEG. Pegylation does not lead to a modification of ultrasonic properties.

Table 5
Quantification of DSPE-PEG in the total suspension, free in the supernatant and associated to MC-PEG, mean of 3 samples per batch (±S.D.).

DSPE-PEG added in the organic phase[a] (μg)	DSPE-PEG in a suspension of MC-PEG[b] (μg)	Free DSPE-PEG[c] (μg)	DSPE-PEG associated to MC-PEG[d] (μg)
44	24.79 ± 4.9	22.41 ± 2.0	2.88 ± 1.0
132	127.0 ± 5.0	99.69 ± 3.7	10.01 ± 0.6
220	227.80 ± 15.3	191.82 ± 27	18.84 ± 2.7

[a] DSPE-PEG corresponding to the volumes of 100, 300 and 500 μL at 440 μg/mL.
[b] Quantification in all the suspensions.
[c] In the supernatant, after centrifugation.
[d] In the pellet, after centrifugation.

3.3. Functionalization of microcapsules by biotinylated phospholipids

To confer specific targeting properties to microcapsules, besides having a stealth system, it is necessary to attach ligands at the microcapsule surface. The model ligand chosen was biotin, because the biotin–streptavidin/neutravidin interactions are known to be very strong, rapid and stable non-covalent biological interactions with a high specificity (affinity constant $K_a \sim 10^{15}$ M^{-1}) [27]. Furthermore coupling targeting ligand to a surface using biotin–streptavidin/neutravidin technology has been widely described with micro and nanoparticles [14,28–31]. In addition, MC-Biot could be a starting point for the binding of a whole series of avidinated compounds.

3.3.1. Effect of DSPE-PEG-biotin amount on microcapsule morphology and size distribution

The range of DSPE-PEG-biotin added in the organic phase varied between 62 μg and 2.5 mg. As this phospholipid has a similar chemical structure as DSPE-PEG, no significant differences in size or morphology of biotinylated microcapsules were expected in comparison with pegylated microcapsules. Optical and fluorescent microscopy images (not shown) show that until 0.250 mg of DSPE-PEG-biotin, the structure of microcapsules was not modified. Since these lipids are not fluorescent, Nile Red was added in the formulation for fluorescent microscopy observations. The phospholipid was supposed to be associated to the shell because as the amount of phospholipid increased, morphology changes were observed as for the other phospholipid-decorated microcapsules. The size of MC-Biot did not change significantly with the different amounts of biotinylated phospholipid, the diameter mean was around 6 μm (Table 2), as for microcapsules decorated with PE-Rhod or MC-PEG.

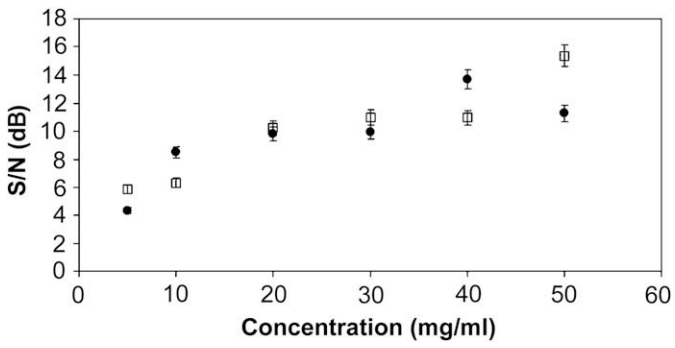

Fig. 8. Signal-to-noise ratio (SNR) of MC (•) and MC-PEG (□) measured at 50 MHz as a function of microcapsule concentration.

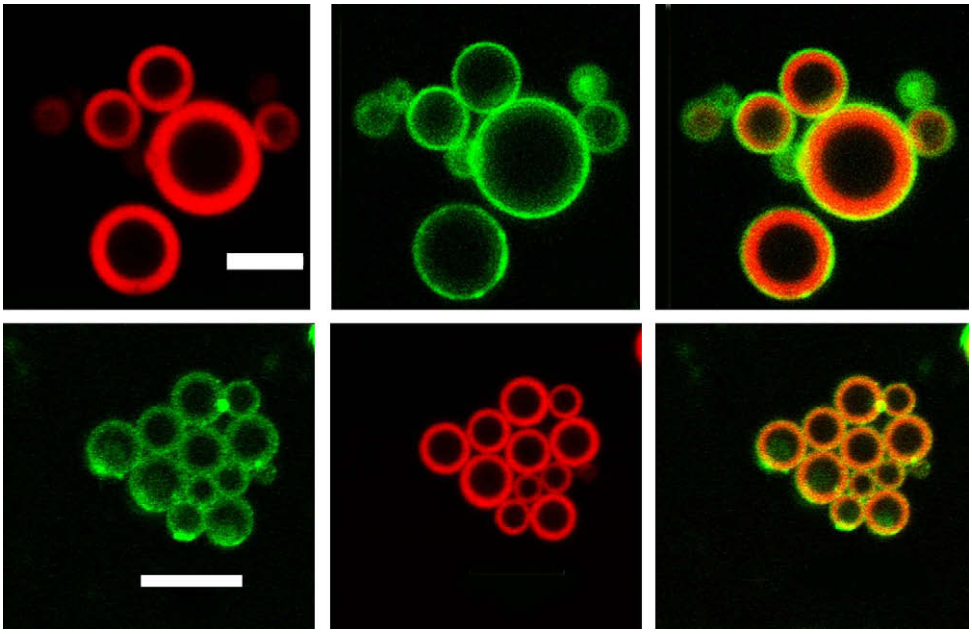

Fig. 9. Confocal microscopy images of a suspension of MC-Biot incubated with fluorescent streptavidin, scale bar = 5 μm (top) and neutravidin, scale bar = 10 μm (bottom). PLGA is dyed in red (left), streptavidin or neutravidin appears in green (center) and superposition of both images (right).

3.3.2. Strepatavidin coupling to MC-Biot

In order to prove that biotin groups were exposed at the surface of microcapsules and accessible to streptavidin, MC-Biot suspensions were incubated with fluorescent streptavidin. Before incubation, it was necessary to estimate the amount of streptavidin necessary to obtain biotin binding. As the chemical structures of DSPE-PEG and DSPE-PEG-biotin are very similar, we considered that 10% of the biotinylated phospholipids added in the organic phase initially were associated to microcapsule surface. It corresponds to a maximum of 4.1×10^{6} biotinylated phospholipids per microcapsule. Considering that a single streptavidin can bind four biotins, the amount of protein necessary to bind all biotin groups present on microcapsule surface in the sample was calculated. 4.1×10^{-8} mmol of streptavidin (2.5 μL at 1 mg/mL) are necessary to bind all the biotins of 100 μL of MC-Biot (equivalent to 1.7×10^{-7} mmol DSPE-PEG-Biot). To ensure that binding was achieved, an excess of fluorescent streptavidin was added and incubated samples were observed by confocal microscopy (Fig. 9). Nile Red was used as a marker for PLGA shell. The shell is well defined and appears in red, while streptavidin appears in green as a thinner layer than the polymeric shell. When the two images are superimposed, the green fluorescence arising from streptavidin fully covers the microcapsule surface, further confirming biotin groups are displayed at microcapsule surface and accessible to streptavidin binding.

Controls were performed to ensure streptavidin was specifically binding to biotinylated microcapsules, using pegylated microcapsules. Because of DSPE-PEG presence, PEG groups should be displayed towards the external aqueous environment forming a hydrophilic steric barrier and preventing streptavidin adsorption. However confocal microscopy images show small green spots of streptavidin on microcapsule surface (not shown). This indicates a non-specific interaction already reported by Weiss et al. [31]. The non-specific interaction of streptavidin can be explained by the orientation of the PEG groups and by the protein charge. Streptavidin is a positively charged glycoprotein with a well-known tendency to non-specific interactions with negatively charged compounds. Since, PLGA microcapsules are negatively charged as attested by Zeta potential measurements [15] the non-specific binding that is observed could arise from electrostatic interactions.

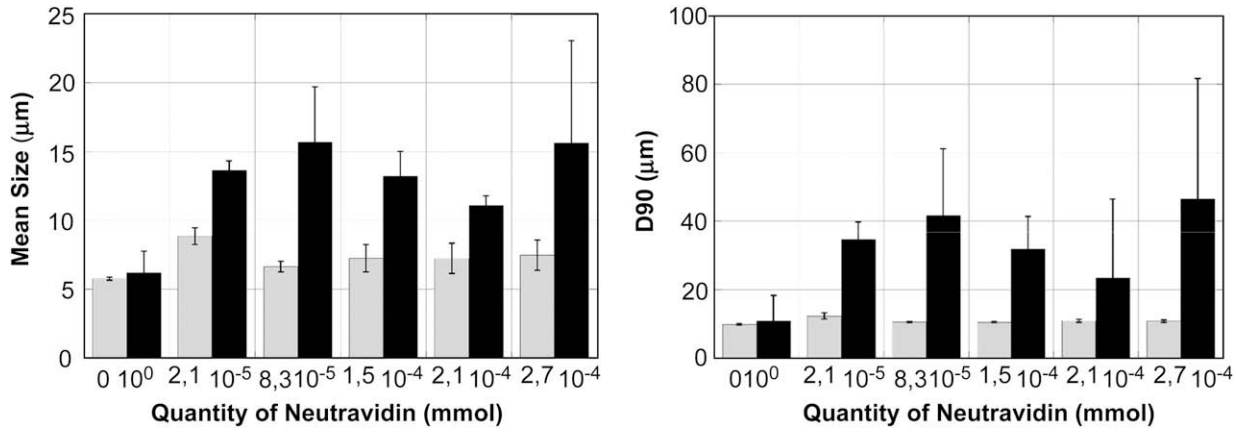

Fig. 10. Mean size (left) and D90 (right) of MC-PEG (in grey) and MC-Biot (in black) incubated with increasing quantities of neutravidin.

In addition the distance between PEG groups could be larger than the size of streptavidin allowing streptavidin to interact with PLGA surface.

Moreover by incubating MC-Biot with increasing amounts of streptavidin, aggregates would be expected to appear, as it has already reported for liposomes and vesicles [32]. Microscopically small aggregates were observable (images not shown) but it was not possible to quantify them by size measurements. Due to the non-specific adsorption of streptavidin onto PLGA surface, streptavidin is hidden by PEG–biotin chains decorating microcapsule surface. The steric barrier formed by these chains reduces the accessibility to streptavidin for biotin groups from other capsules, therefore explaining the small number aggregates present and the difficulty to quantify them.

3.3.3. Neutravidin binding to biotinylated microcapsules

Neutravidin has lower non-specific binding properties due to the absence of carbohydrates, still strong and stable interactions with biotin are maintained [33]. After incubation of fluorescent neutravidin with MC-Biot, aggregates were observed (Fig. 9). As with streptavidin, the fluorescence of the protein is situated at the microcapsule surface proving biotin groups are displayed and accessible. To quantify the aggregation, incubations were performed with increasing amounts of neutravidin with MC-Biot, but also with MC-PEG as a control, and size measurements were performed after each incubation. The mean diameter and D90 were plotted as function of the concentration of neutravidin (Fig. 10). On one hand, for pegylated microcapsules, the mean diameter and D90 were inferior to 10 μm and did not change with increasing neutravidin concentrations. On the other hand, for MC-Biot both diameters increased as a function of neutravidin concentration. The mean diameter increased from 6.1 μm to 15.6 μm, whereas D90 increased from 10 μm to 46.5 μm, confirming the aggregates observed by confocal microscopy. Altogether, microscopic observations and size measurements confirm the presence and accessibility of biotin groups at microcapsule surface, proving the functionalization strategy applied is efficient.

4. Conclusion

The method presented here to modify the surface chemistry of polymeric microcapsules used as ultrasound contrast agents using phospholipids proved to be simple and efficient despite only a 10% of the initial lipids are associated to microcapsules, as quantified by HPLC. The core/shell morphology of microcapsules was preserved up to 0.5 mg fluorescent phospholipids, up to about 0.25 mg pegylated phospholipids or biotinylated phospholipids (for 100 mg PLGA). The presence of pegylated phospholipids at the surface of capsules was confirmed by XPS and confocal microscopy. Pegylation did not modify the echographic signal arising from capsules. Biotinylated microcapsules incubated with neutravidin tended to aggregate, which confirms the presence of biotin groups at the surface of microcapsules. The specific coupling with fluorescent streptavidin/neutravidin was also assessed by confocal microscopy. Results are encouraging and future work with surface modification of nanocapsules is underway. Indeed, functionalized pegylated nanocapsules could be attractive molecularly target contrast agents.

Acknowledgments

Authors acknowledge financial support from CONACYT and Agence Nationale de la Recherche (ANR ACUVA NT05-3-42548). Authors would like to thank E. Pisani for help with microcapsule preparation, A. Allavena-Valette (CECM, Vitry ^{s}/Seine) for access to the SEM facility and M. Besnard for granulometry.

Appendix

Figures with essential color discrimination. Certain parts of the majority of figures in this article are difficult to interpret in black and white. The full colour images can be found in the online version, at doi:10.1016/j.biomaterials.2008.11.032.

References

[1] Straub JA, Chickering DE, Church CC, Shah B, Hanlon T, Bernstein H. Porous PLGA microparticles: AI-700, an intravenously administered ultrasound contrast agent for use in echocardiography. J Control Release 2005;108(1):21–32.
[2] Klibanov AL. Ultrasound molecular imaging with targeted microbubble contrast agents. J Nucl Cardiol 2007;14(6):876–84.
[3] Lindner JR. Microbubbles in medical imaging: current applications and future directions. Nat Rev Drug Discov 2004;3(6):527–33.
[4] Correas JM, Bridal L, Lesavre A, Mejean A, Claudon M, Helenon O. Ultrasound contrast agents: properties, principles of action, tolerance, and artifacts. Eur Radiol 2001;11(8):1316–28.
[5] Weller GE, Wong MK, Modzelewski RA, Lu E, Klibanov AL, Wagner WR, et al. Ultrasonic imaging of tumor angiogenesis using contrast microbubbles targeted via the tumor-binding peptide arginine-arginine-leucine. Cancer Res 2005;65(2):533–9.
[6] Pisani E, Tsapis N, Paris J, Nicolas V, Cattel L, Fattal E. Polymeric nano/microcapsules of liquid perfluorocarbons for ultrasonic imaging: physical characterization. Langmuir 2006;22(9):4397–402.
[7] Pisani E, Tsapis N, Galaz B, Santin M, Berti R, Taulier N, et al. Perfluorooctyl bromide polymeric capsules as dual contrast agents for ultrasonography and magnetic resonance imaging. Adv Funct Mater 2008;18(19):2963–71.
[8] Shive MS, Anderson JM. Biodegradation and biocompatibility of PLA and PLGA microspheres. Adv Drug Deliv Rev 1997;28(1):5–24.
[9] Gref R, Luck M, Quellec P, Marchand M, Dellacherie E, Harnisch S, et al. 'Stealth' corona–core nanoparticles surface modified by polyethylene glycol (PEG): influences of the corona (PEG chain length and surface density) and of the core composition on phagocytic uptake and plasma protein adsorption. Colloids Surf B Biointerfaces 2000;18(3–4):301–13.
[10] Ravi Kumar MN, Bakowsky U, Lehr CM. Preparation and characterization of cationic PLGA nanospheres as DNA carriers. Biomaterials 2004;25(10):1771–7.
[11] Mundargi RC, Srirangarajan S, Agnihotri SA, Patil SA, Ravindra S, Setty SB, et al. Development and evaluation of novel biodegradable microspheres based on poly(D,L-lactide-*co*-glycolide) and poly(epsilon-caprolactone) for controlled delivery of doxycycline in the treatment of human periodontal pocket: in vitro and in vivo studies. J Control Release 2007;119(1):59–68.
[12] Fernandez-Carballido A, Pastoriza P, Barcia E, Montejo C, Negro S. PLGA/PEG-derivative polymeric matrix for drug delivery system applications: characterization and cell viability studies. Int J Pharm 2007.
[13] Muller M, Voros J, Csucs G, Walter E, Danuser G, Merkle HP, et al. Surface modification of PLGA microspheres. J Biomed Mater Res Part A 2003;66A(1):55–61.
[14] Fischer S, Foerg C, Ellenberger S, Merkle HP, Gander B. One-step preparation of polyelectrolyte-coated PLGA microparticles and their functionalization with model ligands. J Control Release 2006;111(1–2):135–44.
[15] Shakweh M, Besnard M, Nicolas V, Fattal E. Poly(lactide-*co*-glycolide) particles of different physicochemical properties and their uptake by Peyer's patches in mice. Eur J Pharm Biopharm 2005;61(1–2):1–13.
[16] Fahmy TM, Samstein RM, Harness CC, Mark Saltzman W. Surface modification of biodegradable polyesters with fatty acid conjugates for improved drug targeting. Biomaterials 2005;26(28):5727–36.
[17] Sakahara H, Saga T. Avidin–biotin system for delivery of diagnostic agents. Adv Drug Deliv Rev 1999;37(1–3):89–101.
[18] Díaz López R, Libong D, Tsapis N, Fattal E, Chaminade P. Quantification of pegylated phospholipids decorating polymeric microcapsules of perfluorooctyl bromide by reverse phase HPLC with a charged aerosol detector. J Pharm Biomed Anal 2008;48(3):702–7.
[19] Pisani E, Fattal E, Paris J, Ringard C, Rosilio V, Tsapis N. Surfactant dependent morphology of polymeric capsules of perfluorooctyl bromide: influence of polymer adsorption at the dichloromethane–water interface. J Colloid Interface Sci 2008;326(1):66–71.
[20] Lichtenberg D, Ragimova S, Bor A, Almog S, Vinkler C, Kalina M, et al. Stability of mixed micellar bile models supersaturated with cholesterol. Biophys J 1988;54(6):1013–25.
[21] Ladaviere C, Tribet C, Cribier S. Lateral organization of lipid membranes induced by amphiphilic polymer inclusions. Langmuir 2002;18(20):7320–7.
[22] Gref R, Minamitake Y, Peracchia MT, Trubetskoy V, Torchilin V, Langer R. Biodegradable long-circulating polymeric nanospheres. Science 1994;263(5153):1600–3.
[23] Owens 3rd DE, Peppas NA. Opsonization, biodistribution, and pharmacokinetics of polymeric nanoparticles. Int J Pharm 2006;307(1):93–102.
[24] Harris JM, Chess RB. Effect of pegylation on pharmaceuticals. Nat Rev Drug Discov 2003;2(3):214–21.
[25] NIST XPS database; 2008.
[26] High resolution XPS of organic polymers: the Scienta ESCA300 database. Chichester: Wiley; 1992.

[27] Green NM. Avidin and streptavidin. Methods Enzymol 1990;184:51–67.
[28] Gref R, Couvreur P, Barratt G, Mysiakine E. Surface-engineered nanoparticles for multiple ligand coupling. Biomaterials 2003;24(24):4529–37.
[29] Duncanson WJ, Figa MA, Hallock K, Zalipsky S, Hamilton JA, Wong JY. Targeted binding of PLA microparticles with lipid–PEG-tethered ligands. Biomaterials 2007;28(33):4991–9.
[30] Nobs L, Buchegger F, Gurny R, Allemann E. Poly(lactic acid) nanoparticles labeled with biologically active neutravidin for active targeting. Eur J Pharm Biopharm 2004;58(3):483–90.
[31] Weiss B, Schneider M, Muys L, Taetz S, Neumann D, Schaefer UF, et al. Coupling of biotin–(poly(ethylene glycol))amine to poly(D,L-lactide-*co*-glycolide) nanoparticles for versatile surface modification. Bioconjug Chem 2007;18(4):1087–94.
[32] Chiruvolu S, Walker S, Israelachvili J, Schmitt FJ, Leckband D, Zasadzinski JA. Higher-order self-assembly of vesicles by site-specific binding. Science 1994;264(5166):1753–6.
[33] Hiller Y, Gershoni JM, Bayer EA, Wilchek M. Biotin binding to avidin. Oligosaccharide side chain not required for ligand association. Biochem J 1987;248(1):167–71.